Serrano-Mislata et al.

Supplementary Methods

DNA constructs and plant transformation*.*

To construct *35SploxGUSloxgaiGFP*, a *gai-GFP* in-frame fusion was amplified from *pGreen0029gaiGFP* [1] with primers 5'-AATTTA**GTCGAC**ATGGATGTTGCTCAGAAACTC-3' and 5'-TAATTT**GGTACC**TTACTTGTACAGCTCGTCCAT-3' , cloned as *Sal*I-*Kpn*I into *pGUSMOS* [2] and the *lox-GUS-lox-gai-GFP* cassette was cloned as *Spe*I-*Kpn*I into *35Sp:lox-GUS-lox-GFP* [2]. To build *35Sp:lox-GFP-lox-GUS*, the *sGFP(S65T)* coding sequence [3] and the *nopaline synthase* (*NOS*) terminator from pCGN18 [4] were cloned between *lox*P sequences [5] as described [2]. The CaMV *35S* promoter [6], *loxGFPnoslox* cassette, *GUS* coding sequence [7] and the *NOS* terminator were then cloned into pZP222 [8] as *EcoRI*-***35Sp***-*Sac*I-*BamHI/Bgl*II-***lox-GFP-nos-lox***-*BamH*I-***GUS***-*Xba*I-***nos***-*Pst*I-*Hind*III. Both *35SploxGUSloxgaiGFP* and *35Sp:lox-GFP-lox-GUS* were transformed into *hsp18.2:Cre* plants by floral dip [9].

For *KRP2p:KRP2-GFP*, a L-*er* genomic fragment of *KRP2* (At3g50630) including 3.6 kb of the 5' promoter region was amplified with primers 5'- AAAA**GGATCC**ACTTGAGAAAGTGATCTGC-3' and 5'-CATCGTCTTCA**CCATGG**ATTCAA-3', replacing the *KRP2* stop codon by a *Nco*I site. 1.3 kb of the *KRP2* 3' promoter region was amplified with primers 5'-TTAA**CTCGAG**T**CCATGG**TGAAGACGATG-3' and 5'-TTTT**GGTACC**TTCTCGCATCTTTGTGTTG-3'. Both *KRP2* genomic fragments were fused at the *Nco*I site in pBluescript KS (-) (Stratagene). The *sGFP(S65T)* coding sequence was amplified with primers 5'-AAAA**CCATGG**GTGAGCAAGGGCGAGGA-3' and 5'-AAAA**CCATGG**CTTGTACAGCTCGTCC-3' and inserted in frame at the *Nco*I site of the *KRP2* construct before cloning *BamH*I/*Kpn*I into pCGN1547 [10]. Wild-type plants of the L-*er* accession

(for expression analysis) and *jag-1 krp2-3* double mutants (for complementation) were transformed as described above.

Vibratome sectioning

Inflorescence tips were fixed with 2.5% (w/v) PFA pH 7.0 in PBS under vacuum for 30 minutes on ice, incubated in fresh 2.5% PFA overnight at 4 °C and washed with a sucrose gradient in 1% PFA solution on ice: 10% sucrose for 20 min, 20% sucrose for 20' and 30% sucrose for 30 min. Tissues were embedded in 7% low melting agarose, 100 μm sections were produced with a 1000 plus vibratome (TAAB) and were collected on microscope slides in 95% PBS/5% glycerol buffer. Imaging was performed with a Zeiss LSM780 confocal microscope and a 10x/0.3 NA objective.

Summarised description of image processing scripts

Python scripts were written in Python 2.7.3 on an Apple computer running MacOS X 10.11.6; dependencies are Numerical Python (http://www.numpy.org), Scientific Python (http://www.scipy.org), matplotlib (http://matplotlib.org) and SimpleITK (http://www.simpleitk.org). The annotated code and instructions are found in the Supplementary Software (DOI: 10.6084/m9.figshare.4675801). A brief description of each script is provided below:

subtract_images.py: used to subtract nuclear signal from the image of cell outlines before segmenting image stacks that include nuclear GFP signal. This prevents over-segmentation artefacts caused by background nuclear signal present in the cell outline image.

median_filter.py: applies a median filter to de-speckle confocal images before segmentation. For this, a region of n * n * n voxels is selected around each voxel and the median value within that region is attributed to the central voxel.

watershed_segmentation.py: applies a Gaussian blur to the image of cell outlines and uses the morphological watershed algorithm [11] implemented in SimpleITK to segment cells in 3D.

double_watershed_segmentation.py: modified version of *watershed_segmentation.py* to improve segmentation of images with loss of intensity along the z axis. An initial segmentation defines cell boundaries, which are used to normalise intensity before a second watershed segmentation.

cell_data_table.py: reads the segmented image and produces a table of comma-separated values with cell data (center of mass, volumes).

rib_zone.py: calculates the distances from the centre of mass of each cell to the main axis or to the apex (defined as a plane normal to the main axis and containing the point where the main axis first crosses the segmented cells) and adds them to the cell data table.

cell_distances.py: similar to *rib_zone.py*, but before distances are calculated, the image is rotated so that the main axis is vertical and runs through the center of the xy plane

score_nuclei.py: normalises GFP signal along the image stack, detects cells with nuclear signal (e.g. GFP), measures signal intensities and adds them to the cell data table.

score_ER.py: similar to score_nuclei.py, but detects cytoplasmic GFP expression.

cell_layers.py: attributes segmented cells to cell layers (1 for epidermis and progressively deeper).

cell_layers_PI.py: modified version of cell_layers.py, used with mPS-PI images to correctly assign cells to L1 even if they are present on juxtaposed surfaces of different organs.

meristem_area.py: delimits the inflorescence meristem based on landmarks placed on the boundaries of floral buds, rotates the image to make the central axis vertical, extracts the voxels on the surface of the meristem, projects them onto a plane and calculates the projected area.

select_ROIs.py: selects regions of interest (ROIs) corresponding to the meristem and buds, using four landmarks; the selected region is the intersection between a sphere containing all landmarks and the region of the image above a best-fitting plane containing the landmark closest to the bottom of the image stack.

find_rib_meristem.py: used to attribute cells to the rib meristem or apical (tunica) layers by detecting tissue regions with consistently thicker walls (intensity of mPS-PI signal) and oriented divisions (based on the orientation of the wall with weakest signal). For both parameters, each cell was given the median value for the cell and its neighbors. Threshold values were optimised by visual inspection for wild-type images and applied uniformly to all genotypes, including cutoffs distances to the meristem summit and to the main axis (Table S4). Processed images were manually curated (using the Fiji macro *correct_segmentation.ijm*, see below) to remove incorrectly attributed cells before statistical analysis (average of 1% and 6% removed for and RM regions, respectively).

slice_meristem.py: selects the meristem in a barley inflorescence apex as the region above a plane fitted to four landmarks, which are placed on the first two (earliest) boundaries of spikelet primordia and on either side of the apex, half way between the boundary points.

cell_stats_batch.py: used to pool data from cell data tables of multiple images; also allows filtering the data based on the range of values for any measurement on the tables. The parameter values used to filter data for each figure are listed in Table S4.

cell_stats_images.py: used to produce images of cells filtered by *cell_stats_batch.py.*

bud_analysis_lib.py: library of functions shared between the scripts above.

Fiji [12] was used to visualise and interact with processed images (e.g. to select landmarks or correct segmentation errors). To facilitate this, the following macros were used, which require the plugins and the plugins 3D Viewer [13] and PointPicker (http://bigwww.epfl.ch/thevenaz/pointpicker/).

confocal_to_TIF.ijm: creates a folder containing cropped TIF stacks for each channel of a confocal image stack the associated metadata.

meristem_threshold_image.ijm: similar to *confocal_to_TIF.ijm*, but in addition uses the Process/Filters/Gaussian Blur and Image/Adjust/Threshold functions of Fiji to produce a solid

image of the tissues, which is used to define the meristem area using the script *meristem_area.py*.

landmarks_3D.ijm: selects an image to be landmarked, opens the Fiji plugin 3D Viewer and provides instructions to produce different sets of landmarks used by the Python scripts listed above.

axis_orthogonal_planes.ijm: uses orthogonal views of the image to specify two planes that intersect to define the main axis of the inflorescence apex.

view_seg.ijm: used to visualise segmented images; opens the 16-bit image, adjusts voxels dimensions, sets the color scheme and displays the image in orthogonal views.

correct_segmentation.ijm: selects a segmented image to correct, overlaps it with the original confocal image to reveal segmentation errors, presents a PointPicker window to select cells to fuse, delete or recover from a previous version of the segmented image, executes the corrections and saves both the original and corrected images.

Supplementary References

1 Fleck, B. & Harberd, N. P. Evidence that the Arabidopsis nuclear gibberellin signalling protein GAI is not destabilised by gibberellin. *Plant J.* **32**, 935-947 (2002).

2 Gallois, J. L., Woodward, C., Reddy, G. V. & Sablowski, R. Combined SHOOT MERISTEMLESS and WUSCHEL trigger ectopic organogenesis in Arabidopsis. *Development* **129**, 3207-3217, doi:Unsp dev0423 (2002).

3 Chiu, W. *et al.* Engineered GFP as a vital reporter in plants. *Curr. Biol.* **6**, 325-330. (1996).

4 Jack, T., Fox, G. L. & Meyerowitz, E. M. Arabidopsis homeotic gene APETALA3 ectopic expression: transcriptional and posttranscriptional regulation determine floral organ identity. *Cell* **76**, 703-716 (1994).

5 Hoess, R. H., Ziese, M. & Sternberg, N. P1 site-specific recombination: nucleotide sequence of the recombining sites. *Proc Natl Acad Sci U S A* **79**, 3398-3402. (1982).

6 Benfey, P. N. & Chua, N. H. The Cauliflower Mosaic Virus 35S Promoter: Combinatorial Regulation of Transcription in Plants. *Science* **250**, 959-966, doi:10.1126/science.250.4983.959 (1990).

7 Jefferson, R. A., Kavanagh, T. A. & Bevan, M. W. GUS fusions: beta-glucuronidase as a sensitive and versatile gene fusion marker in higher plants. *EMBO J.* **6**, 3901-3907 (1987).

8 Hajdukiewicz, P., Svab, Z. & Maliga, P. The small, versatile pPZP family of Agrobacterium binary vectors for plant transformation. *Plant Mol. Biol.* **25**, 989-994 (1994).

9 Clough, S. J. & Bent, A. F. Floral dip: a simplified method for Agrobacterium-mediated transformation of Arabidopsis thaliana. *Plant J.* **16**, 735-743, doi:10.1046/j.1365-313x.1998.00343.x (1998).

10 McBride, K. E. & Summerfelt, K. R. Improved binary vectors for Agrobacterium-mediated plant transformation. *Plant Mol. Biol.* **14**, 269-276 (1990).

11 Soille, P. *Morphological image analysis: principles and applications*. (Springer Science & Business Media, 2013).

12 Schindelin, J. *et al.* Fiji: an open-source platform for biological-image analysis. *Nat. Methods* **9**, 676-682 (2012).

13 Schmid, B., Schindelin, J., Cardona, A., Longair, M. & Heisenberg, M. A high-level 3D visualization API for Java and ImageJ. *BMC Bioinformatics* **11**, 274 (2010).

Supplementary figures and table legends

Fig. S1. DELLA proteins function primarily in the terminal region of the inflorescence stem. (A,B) *GAIp:GUS* (A) and *RGAp:GUS* (B) expression (blue) in inflorescence apices; the arrow indicates the inflorescence meristem (IM), which is surrounded by developing buds. (C) Side view of *GAIp:GUS* inflorescence apex, showing GUS expression in the developing stem. (D) Vibratome section through an inflorescence apex showing *RGAp:GFP-rgaΔ17* expression (green) against auto-fluorescent background (red); the arrow shows the inflorescence meristem (IM). (E) Diagram of Cre-*lox*P constructs used for localised expression; activation of heat shock-inducible Cre recombinase led to expression of GUS (left) or gai-GFP (right) driven by the ubiquitously expressed 35S promoter, due to removal of an intervening *lox*P-flanked reporter (GFP or GUS, respectively). (F) GUS expression in the inflorescence stem after localised activation of Cre by running warm water through a 2 mm sponge placed around the stem; the section on the right shows GUS activation in all tissues within the heat-shocked segment. (G) Diagram showing the position of heat shocked segments along the inflorescence apex, with ink marks to track subsequent growth (top), and histogram showing the average and SD (n = 3) for stem elongation 10 days after activating expression of gai-GFP or GFP as a control (using a *35S:loxGUSloxGFP* line)[35] in each segment. Bars: 1 mm (A-C, F), 100 µm (D).

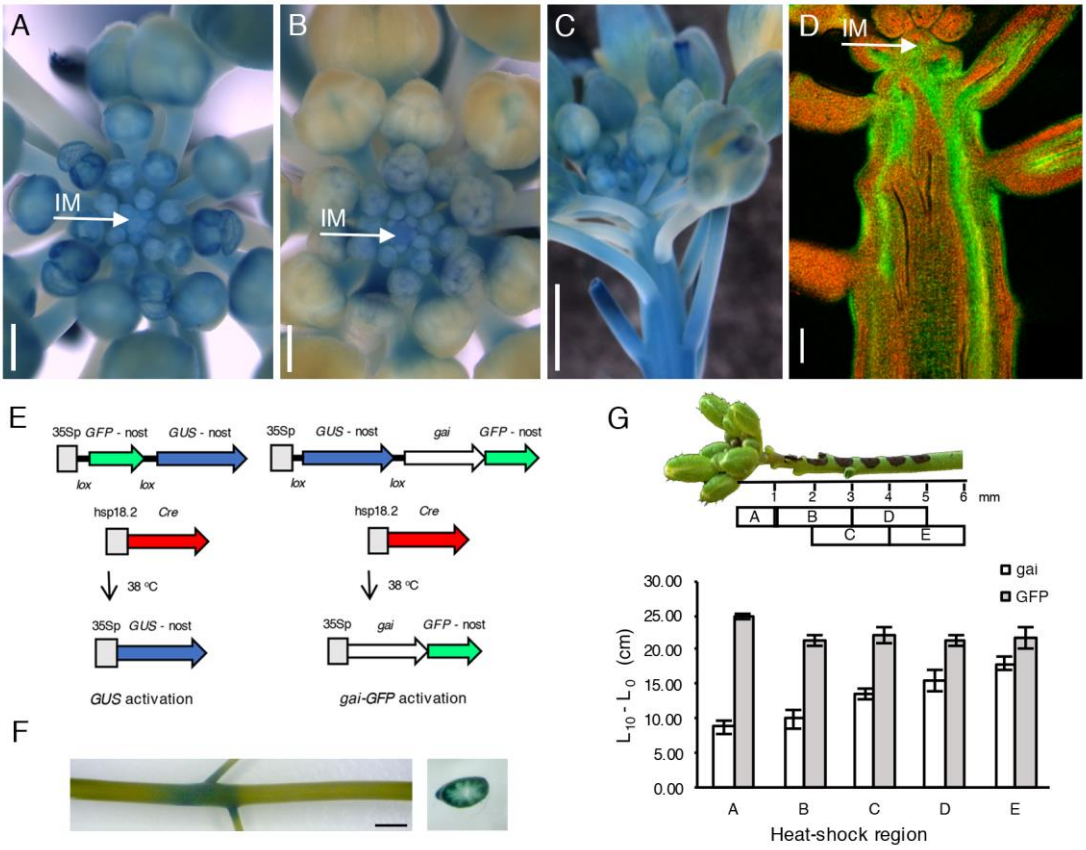
A
IM
B
IM
C
D
IM
E
35Sp GFP - nost
GUS - nost
lox
lox
hsp18.2
Cre
38 °C
35Sp GUS - nost
GUS activation
35Sp GUS - nost
gai
GFP - nost
lox
lox
hsp18.2
Cre
38 °C
35Sp gai GFP - nost
gai-GFP activation
F
G
1 2 3 4 5 6 mm
A
B
C
D
E
gai
GFP
30.00
25.00
20.00
15.00
10.00
5.00
0.00
L10 - L0 (cm)
A
B
C
D
E
Heat-shock region

Fig. S2. DELLA proteins inhibit cell proliferation in developing internodes and appeared to reduce SAM size. (A) 3D reconstruction from confocal sections of a wild-type (L-*er*) inflorescence tip stained by modified pseudo-Schiff propidium iodide (mPS-PI); the SAM and a young bud are indicated; older buds were removed, to reveal nodes (*n,* at the scar where the floral pedicel was attached to the stem) and developing internodes (*i*); the rectangle contains the region shown close-up in (D). (B, C internode cells expressing the mitotic marker *CYCB1;1p:GFP* (green dots, some of which are indicated by arrows) in representative wild-type (B) and *gai* (C) inflorescence apices (3D reconstruction from confocal sections of cleared apices). (D-F) Close-up views of internode regions of inflorescence tips (3D reconstruction from confocal sections after mPS-PI staining) showing similar cell sizes in the wild type (D), *gai* (E) and *RGAp:GFP-rga△17* (F). (G-I) Longitudinal confocal sections of mPS-PI-stained apices of wild-type (G), *gai* (H) and *RGAp:GFP-rga△17* (I) inflorescences; yellow lines separate the tunica and RZ regions. Bars: 100 µm.

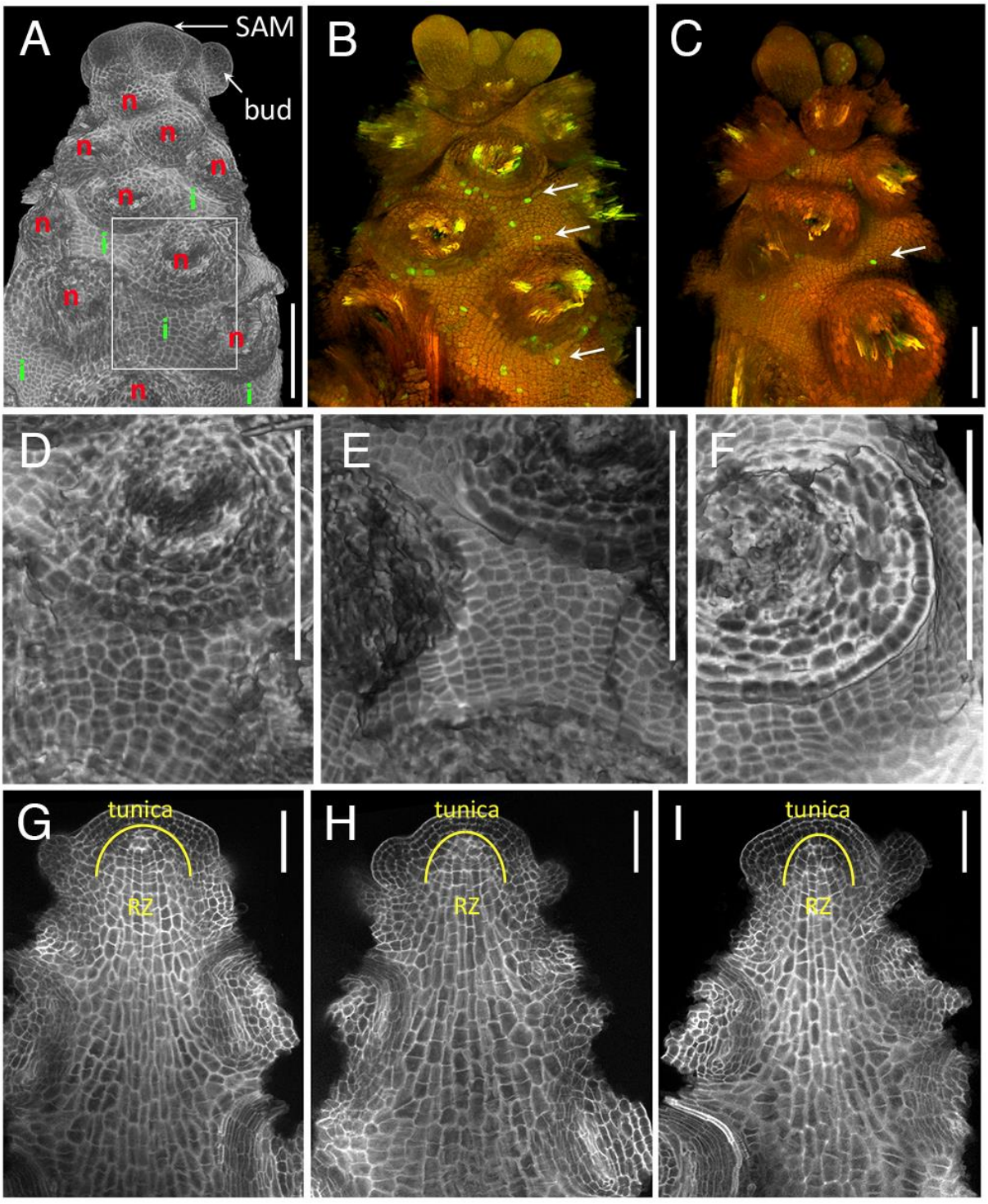
A
SAM
bud
n
i
B
C
D
E
F
G
tunica
RZ
H
tunica
RZ
I
tunica
RZ

Fig. S3: Examples of GFP-rga△17 **ChIP-seq peaks and enrichment of DNA motifs within peak regions.**

A-D) Read frequency histograms showing binding of GFP-rga△17 to (A) *SCL3* (highest-scoring control gene, Table S1), (B) *LFY* (control gene with the lowest score), (C) CLV1 (example of meristem regulatory gene) and (D) FBL17 (example of locus not bound by GFP-rga△17, used as negative control in Fig.2C); "rep.1" to "rep-3" refer to three biological replicates using *RGAp:GFP-rga△17* and wild-type control plants; chromosome position and regions detected as reproducible peaks (blue bars) are indicated at the top; at the bottom, black bars and lines indicate exons and introns, respectively. (E) Enriched motifs detected by MEME-ChIP (http://meme-suite.org/tools/meme-chip)[43] within 75 nt of the center of ChIP-seq peaks for all high-confidence GFP-rga△17 targets (Table S1); only motifs at least 6 nucleotides long and with an E-value of less than 0.001 are shown; families of plant transcription factors that bind to similar motifs are indicated on the right, with specific examples of motifs found in the JASPAR database (http://jaspar.genereg.net/cgi-bin/jaspar_db.pl) within brackets.

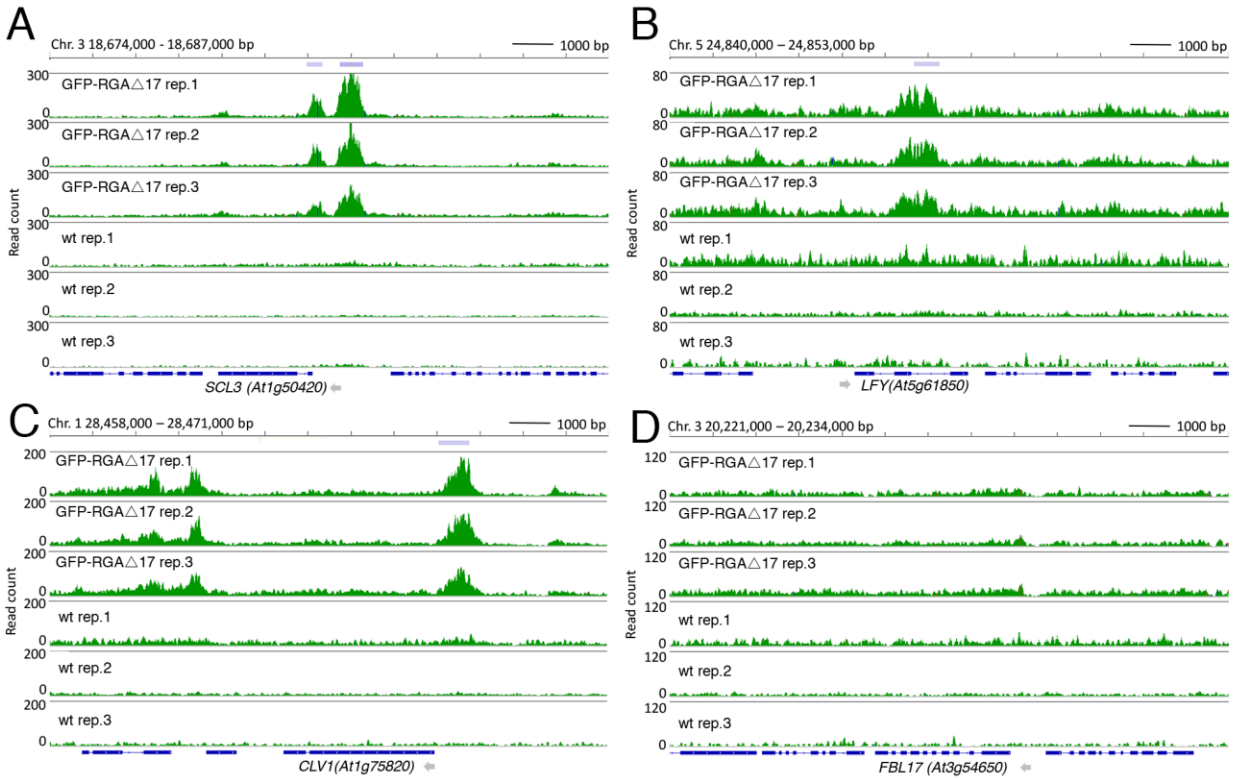

E

Motif found	Discovery/ enrichment program	E-value	Transcription factor families and JASPAR motifs
	DREME	6.7 e-87	bHLH (PIF4 MA0561.1, MYC2 MA0566.1); bZIP (ABI5 MA0931.1, HY5 MA0551.1); BZR1 (MA0550.1)
	MEME	2.9 e-08	
	MEME	4.4 e-74	DOF Zn finger (MA0020.1)
	DREME	8.5 e-05	

Motif found	Discovery/ enrichment program	E-value	Transcription factor families and JASPAR motifs
	DREME	8.3 e-17	WRKY (WRKY12, MA1075.1)
	MEME	8.3 e-010	
	DREME	3.5 e-10	SPL (SPL12 MA1057.1)
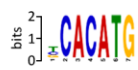	DREME	1.3 e-04	bHLH (PIF4 MA0561.1, PIF5 MA0562.1)

Fig. S4. *KRP2p:KRP2-GFP* complements *krp2-3*. (A-C) The *krp2-3* single mutant has no obvious defects in shoot development because of redundancy with other *KRP* genes, but loss of *KRP2* function is visible in the *jag-1* mutant background as a partial recovery of floral organ growth [18]; in *jag-1 krp2-3* plants transformed with *KRP2p:KRP2-GFP*, floral buds look similar to those of the *jag-1* single mutant, showing that KRP2 function has been restored. (A) Top view of inflorescence apices; arrows point to flowers at comparable developmental stages. (B) Close-up of representative young flowers; note that the partial recovery of sepal and petal growth in *jag-1 krp2-3* flowers was suppressed in *jag-1 krp2-3 KRP2p:KRP2-GFP*. (C) Close-up of representative mature flowers; the narrow sepals seen in *jag-1* flowers were partially restored in *jag-1 krp2-3* but were reverted to a *jag-1*-like phenotype in *jag-1 krp2-3 KRP2p:KRP2-GFP*. Bars: 1 mm.

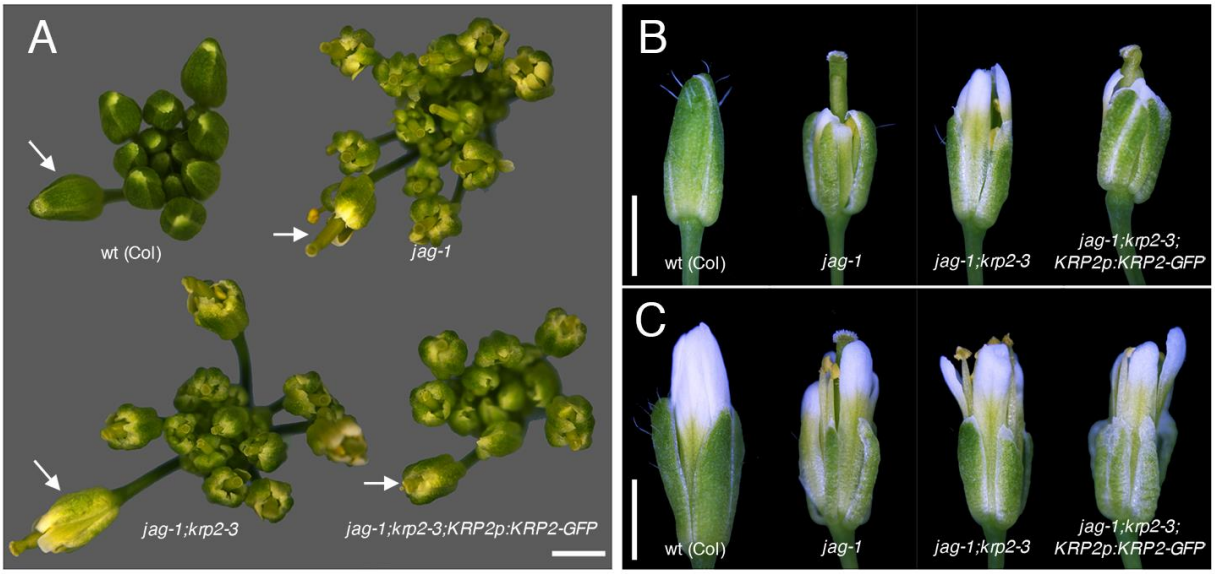
A
wt (Col)
jag-1
jag-1;krp2-3
jag-1;krp2-3;KRP2p:KRP2-GFP
B
wt (Col)
jag-1
jag-1;krp2-3
jag-1;krp2-3;
KRP2p:KRP2-GFP
C
wt (Col)
jag-1
jag-1;krp2-3
jag-1;krp2-3;
KRP2p:KRP2-GFP

Fig. S5. The *krp2* mutation partially suppresses the meristem size defects of *RGAp:GFP-rga△17* and *ga4-1*. (A) 3D reconstructions from confocal images of representative mPs-PI-stained inflorescence apices of wild-type (L-*er*), *krp2-3*, *rga△17* (*RGAp:GFP-rga△17*), *rga△17 krp2-3*, *ga4-1* and *ga4-1 krp2-3* plants. (B) Boxplots of SAM areas measured as in Fig. 1B for the genotypes shown in (A) (10, 8, 10, 8, 9 and 10 plants each for wt, *krp2-3*, *rga△17* t, *rga△17 krp2-3*, *ga4-1* and *ga4-1 krp2-3*, respectively); *p*-values are for equality of means (Student's *t*-test). Bars: 50 µm.

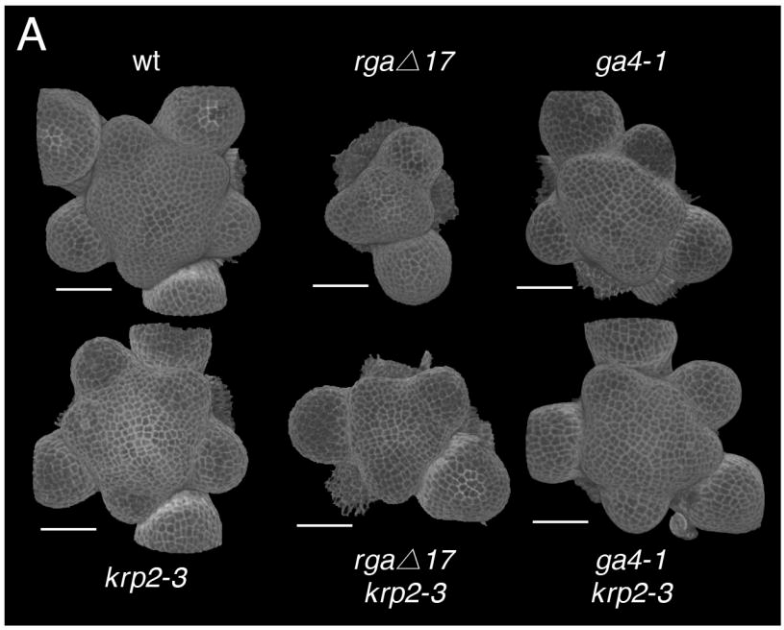
A
wt
rgaΔ17
ga4-1
krp2-3
rgaΔ17
krp2-3
ga4-1
krp2-3

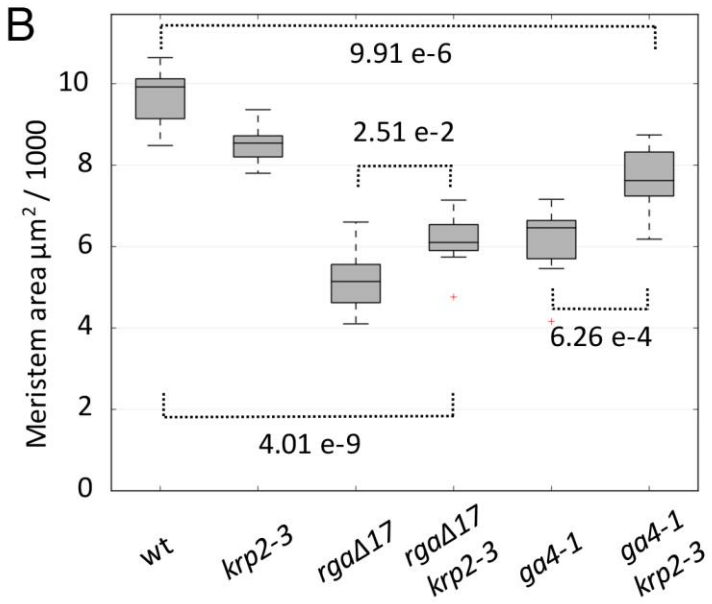
B
9.91 e-6
2.51 e-2
6.26 e-4
4.01 e-9
Meristem area µm² / 1000
0
2
4
6
8
10
wt
krp2-3
rgaΔ17
rgaΔ17 krp2-3
ga4-1
ga4-1 krp2-3

Fig. S6. *gai* did not restrict SAM size by interfering with the *WUS-CLV* regulatory loop. (A-D) Orthogonal views of confocal image stacks showing expression of *WUSp:GFP-WUS* (A,B) or *CLV3p:GFP* (C,D) in wild-type (A,C) and *gai* (B,D) inflorescence apices stained with FM4-64; regions containing detectable GFP signal after 3D segmentation (see Supplementary Information) are shown in cyan and were used to measure the cell numbers and signal intensities shown in (E-H). (E-H) Boxplots showing the number of inflorescence meristem cells with GFP signal (E, G) and the signal intensity per cell (F, H) in wild-type (blue) and *gai* (red) apices comparable to those shown in (A-D). *p*-values are for equality of means (Student's *t*-test) in (E, G) and for equality of medians (Mann-Whitney test) in (F, H), for which the data did not fit a normal distribution (Table S4). Bars: 50 µm (A-D).

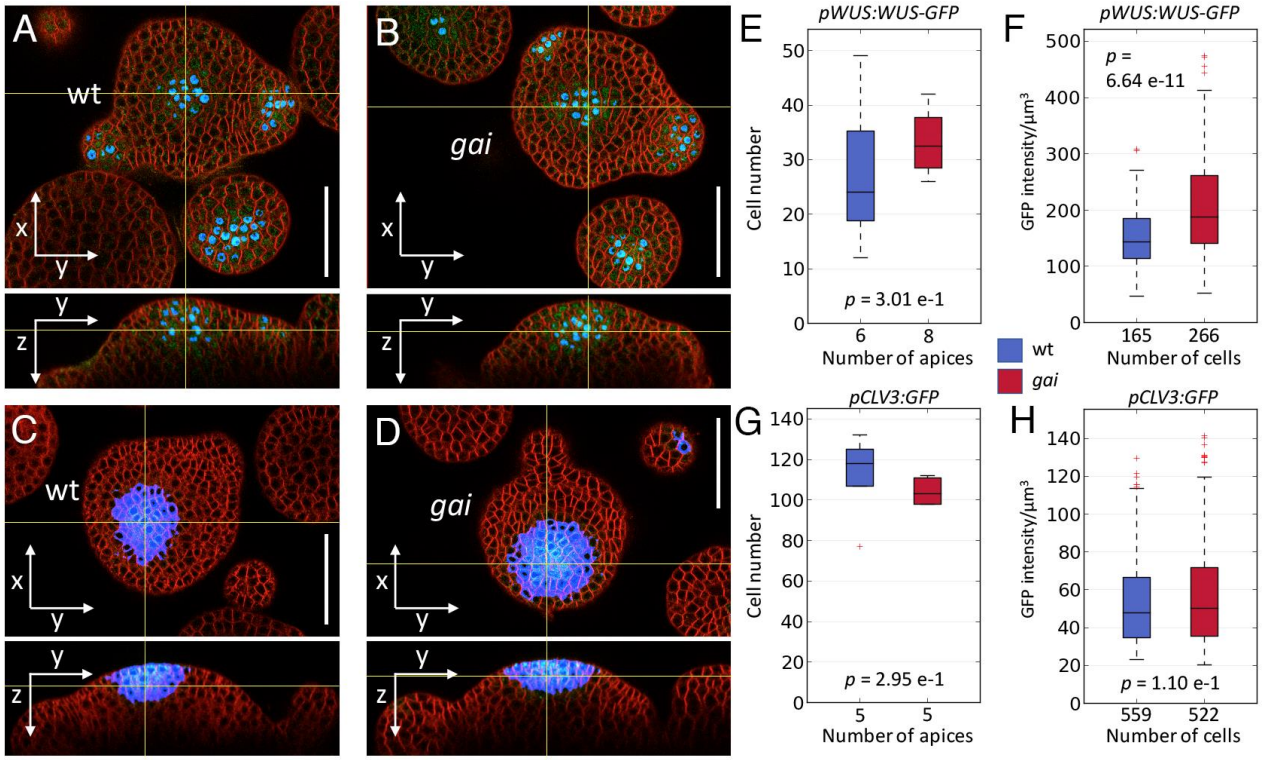

Supplementary table legends

Table S1: High-confidence targets of RGAp:GFP-rga△17 identified by ChIP-seq in inflorescence apices.

Table S2: Manually annotated functional categories of selected RGAp:GFP-rga△17 target genes identified by ChIP-seq in inflorescence apices.

Table S3: Source images and processing steps for data presented in each figure.

Table S4: Imaging data - Filtering parameters, source data and statistical analysis for each figure.

Table S5: ChIP-PCR source data (related to Figure 3C)